Weak Temperature Dependence in the Magnetic Circular Dichroism of Matrix-Isolated Copper Phthalocyanine

Cara L. Dunford and Bryce E. Williamson*

Department of Chemistry, University of Canterbury, Private Bag 4800, Christchurch, New Zealand

Received: August 7, 1996; In Final Form: December 10, 1996[⊗]

Weak temperature dependence is reported for the Q-band magnetic circular dichroism of Cu phthalocyanine in an Ar matrix between 15 and 1.5 K. Moment analysis reveals a zero-field splitting of 1.5 ± 0.5 cm^{-1} in the singdoublet Q state. This is interpreted to be a consequence of interference between spin−orbit coupling and exchange interactions with the tripdoublet state.

I. Introduction

In the 1960s, Buckingham and Stephens developed a theoretical formalism of the Faraday effect,[1−3] which vastly facilitated the utilization of magnetooptical data, particularly magnetic circular dichroism (MCD), in the determination of molecular electronic structure. Among the earliest applications of this formalism Stephens et al.[4] provided an interpretation of magnetooptical data (obtained earlier by Shashoua[5]) concerning porphyrin and phthalocyanine (Pc) systems.

The substantial literature that has since accumulated on the MCD of porphyrins and Pcs has been the subject of several reviews.[6−11] Most of these studies involve the determination of electronic symmetries and angular momenta, and correlations of these properties against central metal ion or substituents. However, when used in conjunction with the method of moments and/or analysis of the spectral dispersion, the technique is capable of much more,[12] for example, the elucidation of vibronic and crystal-field effects.[13−16] For paramagnetic systems, information can also be obtained by following the magnetic-field and temperature dependencies of the MCD. The former has been used in investigations of hemoproteins,[10] but there are surprisingly few examples where the temperature dependence has been utilized.

The most comprehensive spectroscopic temperature-dependence study of porphyrin-related species was conducted by Misener,[17] who surveyed a series of first-row transition-metal phthalocyanines (MPc, with M = Mn to Zn) isolated in Ar matrixes. He measured MCD and absorption spectra at nominal temperatures of 4.2 and 3.0 K. All of the paramagnetic species showed MCD temperature dependence. For MnPc/Ar, this dependence was very strong and was later ascribed to a large magnetic moment associated with a ^4E_g ground-state term.[18] However for CuPc/Ar and CoPc/Ar, the dependence was much weaker, and its origins proved elusive.

For temperature-dependence data to be amenable to quantitative analysis, the temperatures must be accurately known. This is best achieved by immersing the sample in a cryogenic fluid, with which it is at thermal equilibrium. However, the preparation of matrix-isolated samples requires a near vacuum, hence the vast majority of such studies (including Misener's) use samples mounted in vacuum and cooled by conduction through the deposition substrate. The consequent thermal gradients (both within the sample and between the sample and the thermal sensor) are essentially unmeasurable and can lead to substantial thermometry errors. The only documented method of overcoming this problem involves an "injection" technique, where the sample is prepared in a vacuum then rapidly transferred (injected) into a chamber that is immediately flooded with cryogen.[19] Examples of the successful application of the techniques are sparse,[20−22] principally because active cooling of the sample is suspended during injection. Unless the procedure is exceedingly well coordinated, the temperature can rise above ∼30 K, which destroys the sample.

In this work, we report MCD and absorption spectra for the Q($\pi^* \leftarrow \pi$) transition of CuPc isolated in an Ar matrix (CuPc/Ar). As well as conferring beneficial optical properties, matrix isolation precludes axial solvent coordination and circumvents the acute insolubility of CuPc. An improved injection system was employed, where the sample is actively cooled throughout the injection procedure. The weak MCD temperature dependence is confirmed and quantified by using moment analysis. A theoretical explanation for this temperature dependence is discussed.

II. Experimental Section

The matrix injection system is based around three components (Figure 1); an Oxford Instruments Spectromag SM4 cryomagnet, a CF1204 continuous-flow cryostat, and a 1.7-m siphon rod. The SM4 sits on the optical bed of a substantially modified Jasco ORD/UV-5 spectrometer, the base of which has been shortened so that the injection system can be accommodated within the height of the laboratory. The CF1204 is interlocked to the top of the SM4; the sample spaces of the two cryostats are separated by a gate valve and can be independently evacuated. The siphon rod is top-loaded into the CF1204. A c-cut sapphire matrix-deposition window mounted at the end of the rod is actively cooled by drawing liquid helium through the siphon by means of a diaphragm pump.

With the rod retracted and the gate valve closed, the sample is prepared within the CF1204. For the present work, CuPc was sublimed from a quartz Knudsen cell, which was resistively heated to ∼350 °C. The sublimate was co-deposited with Ar gas (∼2 mmol/h) onto the deposition window (∼14 K) to give a sample concentration of ∼2 mol L^{-1} (CuPc:Ar ≈ 1:2000). After matrix preparation, the gate valve is opened and the rod is "injected" slowly into the precooled (∼10 K) sample chamber of the SM4. At the same time, a small space between two sliding seals at the top of the CF1204 is evacuated to prevent air leaks, which can destroy the matrix and block the needle valve of the SM4.

Once the deposition window is positioned in the optical path of the spectrometer, the sample chamber is flooded with liquid

* Corresponding author. E-mail: B.Williamson@chem.canterbury.ac.nz.
[⊗] Abstract published in *Advance ACS Abstracts,* February 15, 1997.

S1089-5639(96)02394-8 CCC: $14.00

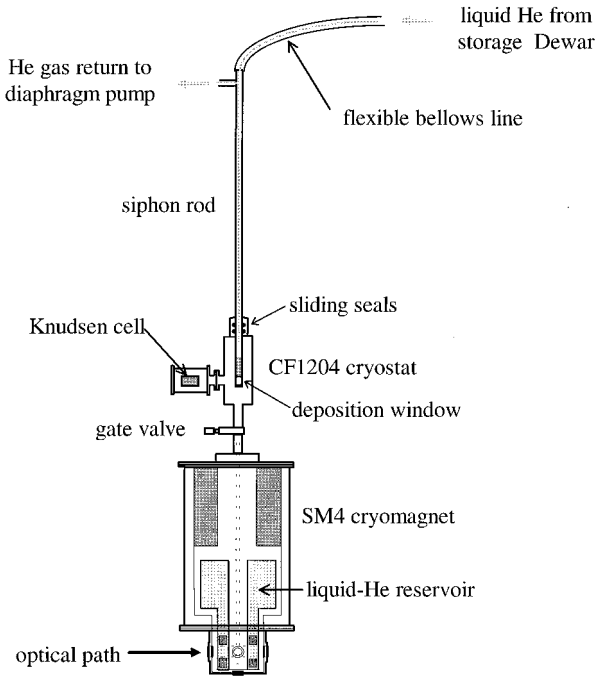

Figure 1. Schematic diagram of the injection system used for measuring temperature-dependent magnetooptical spectra of matrix-isolated systems. The components and their operation are described in section II.

He, which is siphoned via a needle valve from the liquid helium reservoir of the SM4. Temperatures between 4.2 and 1.5 K can then be obtained by pumping the sample chamber while controlling the He vapor pressure with an Oxford Instruments MNT manostat. Higher temperatures are achieved by flowing cold He gas past the sample. Temperatures are determined by measuring the vapor pressure over the liquid and/or measuring the resistance of a calibrated carbon resistor.

Data are collected on a PC-AT computer, which also controls the monochromator. The MCD and absorption spectra were measured simultaneously using an instrumental resolution of ~4.4 nm at 650 nm and magnetic induction of 1 T. The optical quality of the matrix was validated by measuring the natural CD of a solution of Λ-cobalt(III) tris(ethane-1,2-diamine) placed between the sample and the detector.

III. Results

Absorption (A) and MCD (ΔA) spectra of the Q-band of CuPc/Ar over the temperature range 1.5−4.2 K are shown in Figure 2. $Q(0,0)$ is the origin transition; its MCD has the appearance of a positive A term (sigmoidal dispersion with negative lobe at lower energy[12]), which is indicative of positive orbital angular momentum in the excited state. $Q(1,0)$ contains overlapping contributions from many vibrational overtones, while $Q(2,0)$ comprises contributions both from overtones and a separate electronic transition,[13,23] which we denote Q'.

The absorption spectrum is temperature independent, but the magnitude of the MCD increases distinctly with decreasing temperature. To quantify the latter, we employ the spectroscopic moments defined by

$$\mathbf{A}_n = \int (A/E)(E - \bar{E})^n \, \mathrm{d}E \qquad (1)$$

$$\mathbf{M}_n = \int (\Delta A/E)(E - \bar{E})^n \, \mathrm{d}E \qquad (2)$$

E is the photon energy (in cm^{-1}) and $\bar{E}$ is the absorption barycenter defined by $\mathbf{A}_1/\mathbf{A}_0 = 0$. The zeroth moments ($\mathbf{A}_0$ and $\mathbf{M}_0$) of CuPc/Ar are positive and temperature independent. $\mathbf{M}_0$ is relatively small and arises predominantly from the Q' transition;[13] integration over the full region of Figure 2 yields $\mathbf{M}_0/B\mathbf{A}_0 = (1.0 \pm 0.4) \times 10^{-3}\ T^{-1}$, which is reduced by more than an order of magnitude by the exclusion of $Q(2,0)$. $\mathbf{M}_1$ is positive and increases linearly (within experimental uncertainty) with the reciprocal of the temperature. This is illustrated in Figure 3, where the dimensionless ratio $\mathbf{M}_1/\mu_B B\mathbf{A}_0$ is plotted against $1/kT$ (in cm^{-1}) for two samples, over the temperature range 1.5−15 K. B is the induction due to the applied magnetic field, μ_B is the Bohr magneton, and k is Boltzmann's constant.

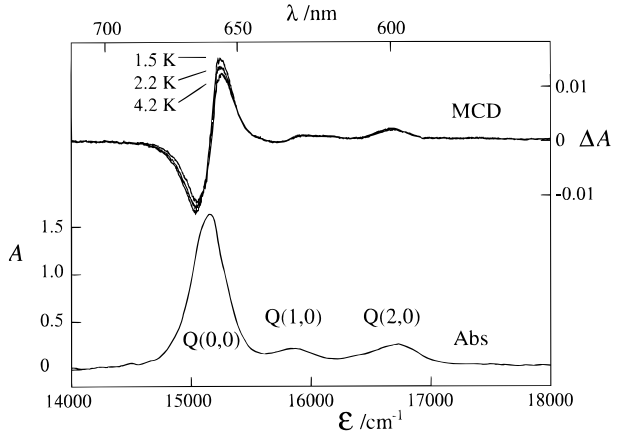

Figure 2. Magnetic circular dichroism (ΔA, top) and absorption spectra (A; bottom) of CuPc/Ar between 4.2 and 1.5 K. The magnetic field is 1 T.

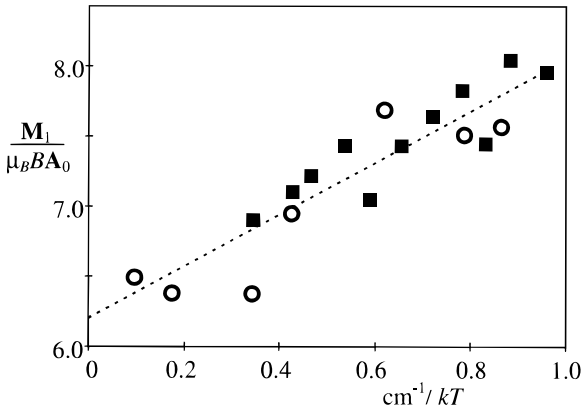

Figure 3. Temperature dependence of the dimensionless moment ratio $\mathbf{M}_1/\mu_B B\mathbf{A}_0$ (obtained by integration over the full range of Figure 2) for two samples of CuPc/Ar. The data represented by squares were obtained from the same sample as Figure 2. The dashed line represents the least-squares fit to all data.

IV. Discussion

Assuming D_{4h} molecular symmetry, CuPc has a $^2B_{1g}$ ground-state term arising from an $a_{1u}^2 b_{1g}$ configuration. The a_{1u} orbital is the π HOMO of the ligand, while b_{1g} is principally of metal $d_{x^2-y^2}$ character.[24] The three lowest-energy ligand-based excited terms arise (predominantly) from the same $e_g(\pi^*) \leftarrow a_{1u}(\pi)$ excitation and are referred to, in order of ascending energy, as the quartet (^4E_u), tripdoublet ($^2E_u^T$) and singdoublet ($^2E_u^S$).[25] ^4E_u and $^2E_u^T$ are essentially single-configuration terms,[24] in which the triplet state of the ligand is coupled with the unpaired b_{1g} electron. $^2E_u^S$ involves the spin singlet of the ligand and contains a significant admixture from $e_g \leftarrow a_{2u}$.[24]

The Q-band arises from fully allowed $x-y$-polarized transitions between the ground state and the two Kramers doublets that constitute $^2E_u^S$. The temperature dependence of $\mathbf{M}_1$ can be

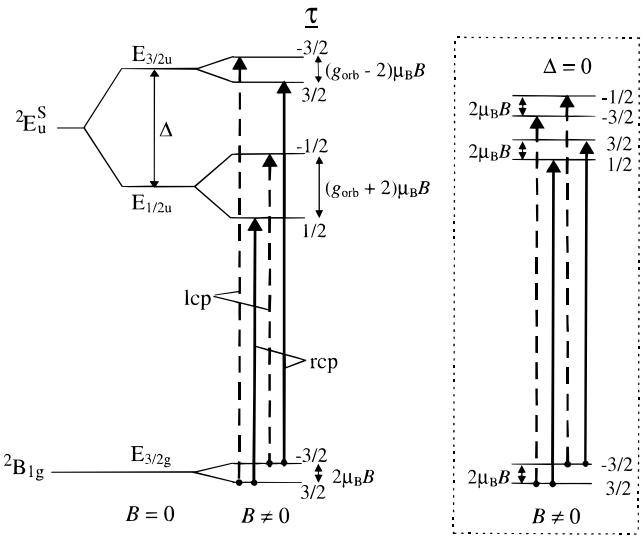

Figure 4. Energy-level diagram for the $^2E_u^S \leftarrow {}^2B_{1g}$ (Q) transition of CuPc/Ar. Parameters and state designations are defined in the text. The Zeeman shifts are given for the case where the applied magnetic field lies along the molecular symmetry axis. Right (rcp) and left circularly polarized (lcp) transitions are respectively indicated by full and dashed lines. The inset illustrates the situation where $\Delta = 0$ and the MCD temperature dependence vanishes.

induced only by effects that separate, but do not mix, the excited-state doublets (vide infra). Thus, for example, even though the $^2E_u^S$ term is susceptible to splitting by low-symmetry crystal-field interactions, such effects have no bearing on the MCD temperature dependence. We therefore regard the chromophore as having exact D_{4h} symmetry and refer to the states by the double-group irrep and partner labels E_t and τ, where $t = {}^1/_2$ or ${}^3/_2$ and $\tau = \pm t$. (In a commonly used alternative notation, E′ $= E_{1/2}$ and E″ $= E_{3/2}$.) The ground state transforms as $E_{3/2g}$, while the excited-state levels are $E_{1/2u}$ and $E_{3/2u}$.

The relevant energy-level diagrams, in both the absence ($B = 0$) and presence ($B \neq 0$) of an external magnetic field, are given in Figure 4. The zero-field splitting of the excited state is denoted Δ:

$$\Delta = E(E_{3/2u}) - E(E_{1/2u}) \tag{3}$$

When a magnetic field is applied the levels split according to the Zeeman effect, as illustrated in Figure 4 for the case where the field is applied along the molecular symmetry axis ($\boldsymbol{B}//z$). g_{orb} is a measure of the excited-state orbital angular momentum:

$$g_{orb} = \mp 2\langle E_{1/2u}\, \pm {}^1/_2 | L_z | E_{1/2u}\, \pm {}^1/_2 \rangle = \mp 2\langle E_{3/2u}\, \pm {}^3/_2 | L_z | E_{3/2u}\, \pm {}^3/_2 \rangle \tag{4}$$

where L_z is the component of the orbital angular momentum operator along z. Figure 4 also shows the four allowed Zeeman transitions and their polarizations for the experimental configuration used in MCD, i.e., where the radiation propagates along the magnetic-field direction. The selection rules (which reflect the 4-fold symmetry of the system) require transitions with $\Delta\tau = 1$ in modulo 4 (${}^3/_2 \rightarrow -{}^3/_2$ and $-{}^3/_2 \rightarrow -{}^1/_2$) to be left-circularly polarized (lcp), while those with $\Delta\tau = -1$ in modulo 4 (${}^3/_2 \rightarrow {}^1/_2$ and $-{}^3/_2 \rightarrow {}^3/_2$) are right-circularly polarized (rcp). The transition bandwidths are far greater than their separations (fwhm ≈ 350 cm^{-1}), so the absorption spectrum is imperceptibly changed by the presence of the field. On the other hand, the consequences of the Zeeman shifts are clearly apparent in the MCD, which is the differential absorption of lcp and rcp light, defined by

$$\Delta A = A_{lcp} - A_{rcp} \tag{5}$$

The temperature dependence of the Q-band MCD can be qualitatively rationalized in terms of eq 5 and Figure 4. The four Zeeman transitions have the same dipole strengths, so their relative intensities are determined by the Boltzmann populations of the ground-state Zeeman levels. Firstly consider the inset to Figure 4, which shows the case where $g_{orb} > 0$ and $\Delta = 0$. The higher-energy transitions are lcp, so the MCD has the overall appearance of a positive A term, with $\mathbf{M}_1 > 0$. However, since the pairs of transitions with the same circular polarization occur at the same energy, their sum (and hence $\mathbf{M}_1$) is temperature *independent*. Next consider the case shown on the left of Figure 4, where $\Delta > 0$. As the temperature is decreased, the intensities of the transitions furthest from the band barycenter are enhanced, and $\mathbf{M}_1$ increases. If the energy order of $E_{1/2u}$ and $E_{3/2u}$ were reversed ($\Delta < 0$), $\mathbf{M}_1$ would *decrease* with cooling. Hence we can conclude that the experimental data (Figure 2 and 3) require $\Delta > 0$.

These considerations are quantified by

$$\frac{\mathbf{M}_1}{\mu_B B \mathbf{A}_0} = c\left(g_{orb} + \frac{\Delta}{kT}\right) \tag{6}$$

where c is an orientation factor. This expression is obtained assuming D_{4h} symmetry and uses the principle that $\mathbf{M}_1$ and $\mathbf{A}_0$ are invariant to unitary transformations of the excited-state basis.[12] The latter point means that eq 6 holds even in the presence of first-order crystal-field and vibronic effects and is precisely the reason that effects that mix $E_{1/2u}$ and $E_{3/2u}$ can be ignored. However, it does require the moments to be carried over the whole transition, including vibrational overtones.[12] The situation is therefore complicated by the presence of the Q' transition, which should be excluded from the analysis.[13] In an attempt to account for this, moment analysis was applied over ranges both including and excluding Q'.

Porphyrin and MPc molecules have previously been found to take preferential orientations in Ar matrixes with their symmetry axes perpendicular to the deposition surface.[13−16,18] In this orientation, $\boldsymbol{B}//z$ and $c = 1$ in eq 6. Assuming the same condition for CuPc, the best-estimate values obtained from moment analysis are $g_{orb} = 4.5 \pm 1.5$ and $\Delta = 1.5 \pm 0.5$ cm^{-1}. The uncertainty in g_{orb} arises predominantly from the variations of integration range, but its value is in accord with that for ZnPc/Ar ($g_{orb} = A_l^z/D_0^z = 4.2$),[13] as expected for an excitation that is essentially localized to the ligand. On the other hand, Δ is quite insensitive to the range of integration, and its uncertainty arises almost exclusively from the scatter of the data (Figure 3). Although the precision is not, at first sight, particularly impressive, it is worthy of note that it is obtained in the presence of a transition bandwidth that is greater by more than 2 orders of magnitude.

For a ^2E term, one might expect Δ to arise predominantly from first-order SO coupling, but such interactions are nonexistent for a pure singdoublet. Explication of the splitting of $^2E_u^S$ therefore requires consideration of coupling with other electronic states, the most important of which are likely to share the same electronic configuration. We now show that Δ can be semiquantitatively accounted for by ignoring configuration interaction and considering coupling between the $a_{1u}b_{1g}e_g$-configuration basis states defined in Table 1.

The effective electronic Hamiltonian employed is

$$H = H_0 + H_{rep} + H_{SO} \tag{7}$$

where the second and third terms represent interelectron

TABLE 1: Basis Functions for the $a_{1u}b_{1g}e_g$ Configuration of CuPc[a]

	Singdoublets
$\lvert(^2E_u^S,^1/_2)\,E_{3/2u}\,^3/_2\rangle$	$-\frac{1}{\sqrt{2}}\left(\lvert a_1^+e_{-1}^-b_1^+\rangle - \lvert a_1^-e_{-1}^+b_1^+\rangle\right)$
$\lvert(^2E_u^S,^1/_2)\,E_{3/2u}\,{-^3/_2}\rangle$	$-\frac{1}{\sqrt{2}}\left(\lvert a_1^+e_{+1}^-b_1^-\rangle - \lvert a_1^-e_{+1}^+b_1^-\rangle\right)$
$\lvert(^2E_u^S,^1/_2)\,E_{1/2u}\,^1/_2\rangle$	$-\frac{1}{\sqrt{2}}\left(\lvert a_1^+e_{-1}^-b_1^-\rangle - \lvert a_1^-e_{-1}^+b_1^-\rangle\right)$
$\lvert(^2E_u^S,^1/_2)\,E_{1/2u}\,{-^1/_2}\rangle$	$\frac{1}{\sqrt{2}}\left(\lvert a_1^+e_{+1}^-b_1^+\rangle - \lvert a_1^-e_{+1}^+b_1^+\rangle\right)$
	Tripdoublets
$\lvert(^2E_u^T,^1/_2)\,E_{3/2u}\,^3/_2\rangle$	$-\frac{1}{\sqrt{6}}\left(2\lvert a_1^+e_{-1}^+b_1^-\rangle - \lvert a_1^-e_{-1}^+b_1^+\rangle - \lvert a_1^+e_{-1}^-b_1^+\rangle\right)$
$\lvert(^2E_u^T,^1/_2)\,E_{3/2u}\,{-^3/_2}\rangle$	$\frac{1}{\sqrt{6}}\left(2\lvert a_1^-e_{+1}^-b_1^+\rangle - \lvert a_1^-e_{+1}^+b_1^-\rangle - \lvert a_1^+e_{+1}^-b_1^-\rangle\right)$
$\lvert(^2E_u^T,^1/_2)\,E_{1/2u}\,^1/_2\rangle$	$\frac{1}{\sqrt{6}}\left(2\lvert a_1^-e_{-1}^-b_1^+\rangle - \lvert a_1^-e_{-1}^+b_1^-\rangle - \lvert a_1^+e_{-1}^-b_1^-\rangle\right)$
$\lvert(^2E_u^T,^1/_2)\,E_{1/2u}\,{-^1/_2}\rangle$	$\frac{1}{\sqrt{6}}\left(2\lvert a_1^+e_{+1}^-b_1^-\rangle - \lvert a_1^-e_{+1}^+b_1^-\rangle - \lvert a_1^+e_{+1}^-b_1^+\rangle\right)$
	Quartets
$\lvert(^4E_u,^1/_2)\,E_{3/2u}\,^3/_2\rangle$	$-\frac{1}{\sqrt{3}}\left(\lvert a_1^+e_{-1}^-b_1^+\rangle + \lvert a_1^-e_{-1}^+b_1^+\rangle + \lvert a_1^+e_{-1}^+b_1^-\rangle\right)$
$\lvert(^4E_u,^1/_2)\,E_{3/2u}\,{-^3/_2}\rangle$	$\frac{1}{\sqrt{3}}\left(\lvert a_1^+e_{+1}^-b_1^-\rangle + \lvert a_1^-e_{+1}^+b_1^-\rangle + \lvert a_1^-e_{+1}^-b_1^+\rangle\right)$
$\lvert(^4E_u,^1/_2)\,E_{1/2u}\,^1/_2\rangle$	$\frac{1}{\sqrt{3}}\left(\lvert a_1^+e_{-1}^-b_1^-\rangle + \lvert a_1^-e_{-1}^+b_1^-\rangle + \lvert a_1^-e_{-1}^-b_1^+\rangle\right)$
$\lvert(^4E_u,^1/_2)\,E_{1/2u}\,{-^1/_2}\rangle$	$\frac{1}{\sqrt{3}}\left(\lvert a_1^+e_{+1}^-b_1^+\rangle + \lvert a_1^-e_{+1}^+b_1^+\rangle + \lvert a_1^+e_{+1}^+b_1^-\rangle\right)$
$\lvert(^4E_u,^3/_2)\,E_{3/2u}\,^3/_2\rangle$	$-\lvert a_1^-e_{+1}^-b_1^-\rangle$
$\lvert(^4E_u,^3/_2)\,E_{3/2u}\,{-^3/_2}\rangle$	$\lvert a_1^+e_{-1}^+b_1^+\rangle$
$\lvert(^4E_u,^3/_2)\,E_{1/2u}\,^1/_2\rangle$	$-\lvert a_1^+e_{+1}^+b_1^+\rangle$
$\lvert(^4E_u,^3/_2)\,E_{1/2u}\,{-^1/_2}\rangle$	$-\lvert a_1^-e_{-1}^-b_1^-\rangle$

[a] Functions are denoted $\lvert(^{2S+1}L,\lvert M_S\rvert)E_t\,\tau\rangle$ and conform to conventions for Butler's $D_4-D_2-C_2$ basis.[29] L is the orbital term symbol (see text) and $\lvert M_S\rvert$ is used to differentiate between functions within the quartet manifold. The right-hand kets are Slater determinants; parity labels are omitted from a_{1u} and b_{2g} and replaced by the appropriate partner label (±1) for e_g. The spin states ($m_s = \pm^1/_2$) are indicated by superscripts.

repulsion and SO coupling, respectively. The corresponding Hamiltonian matrix factors into blocks according to E_t and τ, the elements of which are given by Table 2. E_q is the average configurational energy, and K_{ae}, K_{ab}, and K_{eb} are exchange integrals; for example

$$K_{ae} = (a_{1u}e_g|e_g a_{1u}) = \int\int a_{1u}^*(1)\, e_g^*(2)\, H_{rep} e_g(1)\, a_{1u}(2)\, d\tau_1\, d\tau_2 \quad (8)$$

Z is a measure of the SO coupling for an e_g electron:

$$Z = \sum_k \langle e_{+1}|\xi_e(k) l_z(k)|e_{+1}\rangle \quad (9)$$

where $l_z(k)$ is the z-component operator for the orbital angular momentum of the electron about nucleus k, $\xi_e(k)$ is the corresponding SO coupling coefficient, and the sum is carried over all nuclei.

Within this model, Δ arises directly from the elements of Table 2 that couple the singdoublet and tripdoublet states. In the context of the current problem, the critical property of these elements is that they involve interference between SO and exchange terms, and this interference is different for $E_{3/2u}$ and $E_{1/2u}$. Prediction of the sign of Δ is simply a matter of deciding the sense (constructive or destructive) of this interference for each, as follows:

(i) Exchange integrals are intrinsically real and positive, and hence the sign of the exchange term is determined by the relative magnitudes of K_{ab} and K_{eb}. Electron density associated with the b_{1g} orbital is confined to the Cu ion and the directly coordinated pyrrole N atoms. The e_g orbital has density on the same atoms, whereas the a_{1u} orbital does not;[24] hence $K_{ab} < K_{eb}$ and the off-diagonal exchange interaction is negative.

(ii) McClure has shown that SO coupling in planar $\pi(p_z)$ molecules (such as free-base porphyrins) must be weak.[26] For metalloporphyrins and MPcs however, a relatively large one-center contribution can arise from $\pi-d$ mixing. In the case of the e_g MO, this involves the metal d_{xz} and d_{yz} orbitals, for which the contribution to Z is

$$Z_d = |c_d|^2 \zeta_d \langle d_{+1}|l_z(Cu)|d_{+1}\rangle \quad (10)$$

c_d is the amplitude of the d-orbital contribution to the molecular orbital, and ζ_d is the SO coupling constant for a Cu^{2+} 3d electron ($\zeta_d \approx 830$ cm^{-1}).[25] Since all factors on the right of eq 10 are positive, $Z_d > 0$.

Applying these results (with appropriate t values) to Table 2, it obtains that interference is constructive for $E_{3/2u}$ and destructive for $E_{1/2u}$. Consequently, $E_{3/2u}$ lies at higher energy and $\Delta > 0$, in agreement with experiment.

Theoretical estimation of the magnitude of Δ is a much more difficult proposition since appropriate parameters of demonstrable reliability are not available for CuPc. Nevertheless, we now show that the experimental value can reasonably be considered in accord with theoretical expectations. Ake and Gouterman[25] have estimated exchange parameters for a generic Cu porphyrin on the basis of an extended Hückel calculation, viz. $K_{ae} = 2605$ cm^{-1}, $K_{eb} = 95.5$ cm^{-1}, and $K_{ab} = 396$ cm^{-1}.

TABLE 2: Matrix Elements for the $E_t\,\tau$ Block of the Effective Hamiltonian for the $a_{1u}b_{1g}e_g$ Configuration of CuPc[a]

	$(^2E_u^S,^1/_2)\,E_t\,\tau$	$(^2E_u^T,^1/_2)\,E_t\,\tau$	$(^4E_u,^1/_2)\,E_t\,\tau$	$(^2E_u,^3/_2)\,E_t\,\tau$
$(^2E_u^S,^1/_2)\,E_t\,\tau$	$E_q + 3K_{ae}/2$	$\sqrt{3}(K_{ab} - K_{eb})/2 - (t-1)Z/\sqrt{3}$	$\sqrt{2}(t-1)Z/\sqrt{3}$	
$(^2E_u^T,^1/_2)\,E_t\,\tau$	$\sqrt{3}(K_{ab} - K_{eb})/2 - (t-1)Z/\sqrt{3}$	$E_q + K_{ab} + K_{eb} - K_{ae}/2 - 2(t-1)Z/3$	$-\sqrt{2}(t-1)Z/3$	
$(^4E_u,^1/_2)\,E_t\,\tau$	$\sqrt{2}(t-1)Z/\sqrt{3}$	$-\sqrt{2}(t-1)Z/3$	$E_q - (K_{ab} + K_{eb} + K_{ae})/2 - (t-1)Z/3$	
$(^4E_u,^3/_2)\,E_t\,\tau$				$E_q - (K_{ab} + K_{eb} + K_{ae})/2 - (t-1)Z$

[a] Basis functions are given in Table 1: $t = ^1/_2$ or $^3/_2$ and $\tau = \pm t$. Parameters are defined in the text.

They also suggest $Z_d = 3.5\ cm^{-1}$ (based on $|c_d|^2 = 4.3 \times 10^{-3}$), which gives $\Delta \approx 0.2\ cm^{-1}$, an order of magnitude smaller than the experimental value. On the other hand, a semiempirical SCF-MO calculation specific to CuPc yields $|c_d|^2 = 1.7 \times 10^{-2}$,[24] which in turn gives $Z_d \approx 15\ cm^{-1}$ and $\Delta \approx 0.9\ cm^{-1}$, within a factor of 2 of the observed value.

There are other effects (including configuration interaction) that could potentially have a bearing on Δ and bring the theoretical value into closer agreement with experiment. To speculate on their importance is of dubious worth in the absence of reliable theoretical parameters. However, we can show that three-center SO coupling terms of the type described by McClure[26] are unlikely to contribute significantly, even though the molecule contains the relatively heavy Cu nucleus. The most important of these terms arises from the fact that electron dynamics responsible for g_{orb} occur in the field of the central metal ion. An estimate for the corresponding contribution to Z can be obtained by considering the e_g molecular orbital as a quasi-atomic orbital of Cu. This gives

$$Z_\pi \approx S_\pi \xi_d \frac{g_{orb}}{2} \frac{\langle r_\pi^{-3} \rangle}{\langle r_d^{-3} \rangle} \tag{11}$$

The distances of the 3d and $e_g(\pi)$ electrons from the Cu nucleus are, respectively, denoted r_d and r_π. $\langle r_d^{-3} \rangle = 55.8\ Å^{-3}$,[27] and we estimate $\langle r_\pi^{-3} \rangle \approx 0.0441\ Å^{-3}$ from molecular-orbital coefficients for e_g.[24] S_π is a screening factor, which takes into account the presence of other Cu and Pc electrons. Setting $S_\pi = 1$ yields an upper limit for Z_π of $1.6\ cm^{-1}$. In fact S_π is certainly very much less than unity, so we can safely presume $Z_\pi \ll 1.6\ cm^{-1}$, and that three-center SO contributions are of no consequence in determining Δ.

Finally, we note that the experimental Δ value reported here represents a lower limit since deviations from exact preferential orientation will decrease the value of c in eq 6, to a minimum of 0.5 for random orientation. However, there are two points that suggest that the CuPc molecules are preferentially oriented to a high degree. First, this has consistently been the experience for metalloporphyrins and MPcs isolated in Ar;[13−16,18] second, $g_{orb} \approx 4.5$ accords closely with previous results for a wide range of MPcs, where g_{orb} is found to fall within the range from ∼3 to 4.6.[13,28] In the case of ZnPc/Ar, the existence of orientational effects was confirmed by monitoring the z-polarized B_3 absorption band (near 310 nm) as the deposition window was rotated by ∼30° with respect to the optical path.[13] In the case of CuPc/Ar, we were unable to observe an equivalent of the B_3 band. However, rather than concluding that the CuPc molecules were randomly oriented, we suspect that this result indicates that the B_3 transition is strongly dependent on the metal ion.

V. Conclusion

We have described a matrix injection apparatus, which allows matrixes to be prepared in vacuum before being immersed in liquid He. The sample is actively cooled throughout the injection procedure, which vastly reduces the risks of thermal destruction of the sample. Using this equipment, we have measured the MCD temperature dependence of copper phthalocyanine isolated in solid Ar. Moment analysis of the spectra reveals a zero-field splitting for the singdoublet Q state of $\Delta = 1.5 \pm 0.5\ cm^{-1}$. This splitting is interpreted as a consequence of interference between spin−orbit coupling and exchange interactions with the tripdoublet term. This work demonstrates the utility of temperature-dependent MCD for providing information about weak perturbations in the presence of very much greater transition bandwidths.

Acknowledgment. The research was conducted with support from the New Zealand Lottery Grant Board, Grant GR 2224987.

References and Notes

(1) Buckingham, A. D.; Stephens, P. J. *Annu. Rev. Phys. Chem.* **1966**, *17*, 399−432.
(2) Stephens, P. J. *J. Chem. Phys.* **1970**, *52*, 3489−3516.
(3) Stephens, P. J. In *Advances in Physical Chemistry*; Prigogine, I., Rice, S. A., Eds.; John Wiley and Sons: New York, 1974; Vol. 35, pp 197−264.
(4) Stephens, P. J.; Suëtaka, W.; Schatz, P. N. *J. Chem. Phys.* **1966**, *44*, 4592−4602.
(5) Shashoua, V. E. *J. Am. Chem. Soc.* **1965**, *87*, 4044−4048.
(6) Sutherland, J. C. In *Pophyrins*; Dolphin, D., Ed.; Academic Press: New York, 1978; Vol. 3, pp 225−248.
(7) Holmquist, B. In *Pophyrins*; Dolphin, D., Ed.; Academic Press: New York, 1978; Vol. 3, pp 249−270.
(8) Goldbeck, R. A. *Acc. Chem. Res.* **1988**, *21*, 95−101.
(9) Stillman, M. J.; Nyokong, T. In *Phthalocyanines Properties and Applications*; Leznoff, C. C., Lever, A. B. P., Eds.; VCH Publishers, Inc: New York, 1989; Chapter 3, pp 133−257.
(10) Cheeseman, M. R.; Greenwood, C.; Thompson, A. J. *Adv. Inorg. Chem.* **1991**, *36*, 201−255.
(11) Stillman, M. J. In *Phthalocyanines. Properties and Applications*; Leznoff, C. C., Lever, A. B. P., Eds.; VCH Publishers: New York, 1993; Vol. 3.
(12) Piepho, S. B.; Schatz, P. N. *Group Theory in Spectroscopy with Applications to Magnetic Circular Dichroism*; Wiley: New York, 1983.
(13) VanCott, T. C.; Rose, J. L.; Williamson, B. E.; Boyle, M. E.; Misener, G. C.; Schrimpf, A. E.; Schatz, P. N. *J. Phys. Chem.* **1989**, *93*, 2999−3011.
(14) Metcalf, D. H.; VanCott, T. C.; Snyder, S. W.; Schatz, P. N.; Williamson, B. E. *J. Phys. Chem.* **1990**, *94*, 2828−2832.
(15) VanCott, T. C.; Koralewski, M.; Metcalf, D. H.; Schatz, P. N.; Williamson, B. E. *J. Phys. Chem.* **1993**, *97*, 7417−7426.
(16) Gasyna, Z.; Metcalf, D. H.; Schatz, P. N.; McConnell, C. L.; Williamson, B. E. *J. Phys. Chem.* **1995**, *99*, 5865−5872.
(17) Misener, G. C. Ph.D. Thesis, University of Virginia, Charlottesville, VA, 1987.
(18) Williamson, B. E.; VanCott, T. C.; Boyle, M. E.; Misener, G. C.; Stillman, M. J.; Schatz, P. N. *J. Am. Chem. Soc.* **1992**, *114*, 2412−2419.
(19) Krausz, E.; McDonald, P. *J. Phys. E: Sci. Instrum.* **1978**, *11*, 801−804.
(20) Krausz, E. R.; Mowery, R. L.; Schatz, P. N. *Ber. Bunsen-Ges. Phys. Chem.* **1978**, *82*, 134−136.
(21) Rose, J. L.; Smith, D.; Williamson, B. E.; Schatz, P. N.; O'Brien, M. C. M. *J. Phys. Chem.* **1986**, *90*, 2608−2615.
(22) Krausz, E.; Riesen, H.; Schatz, P. N.; Gasyna, Z.; Dunford, C. L.; Williamson, B. E. *J. Lumin.* **1996**, *66*, 19−24.
(23) Huang, T. H.; Rieckhoff, K. E.; Voigt, E. M. *J. Chem. Phys.* **1981**, *85*, 3322−3326.
(24) Henriksson, A.; Roos, B.; Sundbom, M. *Theor. Chim. Acta* **1972**, *27*, 303−313.
(25) Ake, R. L.; Gouterman, M. *Theor. Chim. Acta* **1969**, *15*, 20−42.
(26) McClure, D. S. *J. Chem. Phys.* **1952**, *20*, 682−686.
(27) Fraga, S.; Karwowski, J.; Saxena, K. M. S. *Handbook of Atomic Data*; Elsevier Scientific Publishing Co.: Amsterdam, 1976.
(28) Stillman, M. J.; Thomson, A. J. *J. Chem. Soc., Faraday Trans. 2* **1974**, *70*, 805−814.
(29) Butler, P. H. *Point Group Symmetry Applications: Methods and Tables*; Plenum Press: New York, 1981.